An ultrasound image navigation robotic prostate brachytherapy system based on US to MRI deformable image registration method

Shihui Zhang[1] **PhD,**
Shan Jiang[1] **PhD,**
Zhiyong Yang[1] **PhD,**
Ranlu Liu[2] **PhD,**
Yunpeng Yang[1] **MS,**
Honghua Liang[1] **MS**

1. Tianjin University, Center for Advanced Mechanisms and Robotics, School of Mechanical Engineering, Tianjin, China, 300072
2. Tianjin Institute of Urology& Department of Urology, Second Hospital of Tianjin Medical University, 23 Pingjiang Road, Hexi District, Tianjin, China, 300211

Keywords: -Prostate brachytherapy -Ultrasound probe registration -Deformable registration method -MCC -Ultrasound -Magnetic resonance imaging

Corresponding author:
Shan Jiang PhD, Tianjin University, Center of Advanced Mechanisms and Robotics, School of Mechanical Engineering, 92 Weijin Road, Nankai District, Tianjin, China, 300072,
Tel: +86 13212154030;
Fax: +86-022-27401042;
shanjmri@tju.edu.cn

Received:
9 September 2016
Accepted revised:
29 October 2016

Abstract

Objective: This paper describes an ultrasound image navigation robotic prostate brachytherapy system. It uses a 2D ultrasound (US) probe rigidly fixed to a robotic needle insertion mechanism. Combined with the US probe registration and image registration, this system will help to navigate the prostate brachytherapy to increase the inserting accuracy. **Subjects and Methods:** The novelty of the system is that after the US probe registration using an improved iterative closest point (ICP) registration method, the initial registration for the magnetic resonance imaging (MRI) and US image can be completely automatically. Moreover, a deformable registration method based on statistical measurement was proposed to register US to MRI images intra-operatively. **Results:** The 6-degree of freedom (6-DOF) of robot and ultrasound probe are calibrated together with an accuracy of 0.9mm, allowing the needles to be precisely inserted to the seed targets after the image registration. Experiments were conducted by using US/MRI images ,capturing from patients. Results showed that the accuracies of probe registration and US-MRI registration were: 0.44± 0.12mm and 2.30±0.41mm, respectively. **Conclusion:** With the help of this robotic system, the accuracy and the costing of time for prostate brachytherapy will greatly improve.

Hell J Nucl Med 2016; 19(3): 223-230 *Epub ahead of print: 8 November 2016* *Published online: 10 December 2016*

Introduction

Prostate cancer is now the most commonly diagnosed non-skin malignancy and is the main cause of cancer-related death in men. For example, in the USA, there will be 233,000 new cases of prostate cancer in 2014, accounting for more than a quarter of all new (non-skin) cancer diagnoses of men, and 29,480 deaths from prostate cancer [1].

A number of treatment options are available, depending on a patient's age, medical history, and anatomy, as well as on the stage of the cancer. The most widely used treatment method among the available options is the permanent low-dose rate (LDR) brachytherapy which is a technique that involves the localized irradiation of the prostate by the permanent insertion of about 100 tiny radioactive seeds. Traditionally, the operators take the brachytherapy operation by using ultrasound (US) image to navigate it on the manual device. In order to increase the accuracy, stability, repeatability and dexterity of the surgery, there are many robotic prostate brachytherapy systems designed to help surgeons. Yu et al. (2010) designed and fabricated a device including Transrectal Ultrasonography (TRUS) driver, gantry robot, needle inserter and a modular robotic platform for positioning the needle [2, 3], fitted to a cart with electronic housing, to perform minimally invasive interventions in prostate brachytherapy [4-6]. Other researchers [7] developed a 6-DOF robot accomplished by 3 translating stages, 2 rotating joints and a needle rotation device, with the electromagnetic tracking system aimed to monitor transperineal needle placement in prostate brachytherapy. Other researchers [8-10] have also designed a robotic assistant system for US guided prostate brachytherapy, in which the puncture needles operated manually by a needle template.

Most of these robotic prostate brachytherapy systems use US images to navigate the operation process. However, the poor quality of the US image makes it not sufficient as a navigation method. In recent years, there are many scholars doing research on how to improve the quality of the US image and reach a consensus on the best way to use medical image registration.

Medical image registration is the process of spatially aligning images in a common

coordinate space and aligning related features which exist in all images. This issue has been a widely investigated area in the past few decades, however remains challenging in particular for multi-modal registration. Often, different modalities complement each other well, which is relevant to a vast range of clinical applications for improving diagnosis, treatment planning, interventions, procedure follow-up, and screening. Many prostate minimally invasive surgeries motivate this work, magnetic resonance imaging (MRI) provides a good visualization of the anatomy and tumors, while US is inexpensive and allows for intra-operative use to detect and correct for prostate deformation. Registering US and MRI images is a complex and difficult process, largely because represents information from very different physical properties. Besides, when using the US probe to take an image, the organs deform under the pressure of the probe. In order to register US and MRI images more accurately, deformable image registration (DIR) methods are proposed.

In modern image-guided online and off-line adaptive radiation therapy, deformable image registration is a vital component which can establish a precise correspondence of two images which were collected with different image modalities or at different time voxel-to-voxel [11, 12]. The deformation vector field (DVF) which is the established correspondence by DIR has many applications in radiotherapy. For example, it can be used to promote auto-segmentation for tissue or organ changes in anatomy [13-18], assist to reconstruct high quality CBCT or 4D-CT images [19, 20], calculate accumulated dose in brachytherapy surgery [21-23], estimate organ motion [24-27] etc.

In the past few years, DIR has been investigated in detail and many new improved algorithms have been presented. Kim et al. (2010) proposed a B-spline algorithm whose objective function combined organ contours and depicted manually particular points [28, 29]. Besides, a contour rigidity constraint was implemented into an adaptable Demons algorithm to instruct its objective function [30]. Schreibmann et al (2006)proposed a method that using mapped control volumes to improve the B-spline deformable calculation [31]. However, since the DIR calculation needed a lot of time, the real-time registration of the US image usually used rigid transformation [32] and a mutual information (MI) based registration [33].

In this paper, we propose a robotic prostate brachytherapy system which includes robot parts and image guided brachytherapy system (IGBS). In our system, we use the US image as the navigation method through registered US and MRI images, which applies automatic pre-registration, replaces manual pre-registration after the probe working space calibration and applies a more efficient deformation and registration method than the MI registration.

Subjects, Materials and Methods

System's description

General layout

There are two main parts in our robotic prostate brachytherapy system, which are shown in Figure 1. The first part is the surgical robot which contains two sections (Figure 1), the lower layer is a positioning module and the upper one is an actuating robot. The positioning platform is at the top of the base support stands demanded to have the vertical and horizontal motions automatically actuated. The actuating robot is mounted on the positioning platform, consisting of an US probe holder and a guided module in a similar configuration to the conventional brachytherapy. The robot can manipulate the guided module to be manually translated to appropriate positions and rotated to proper angles in order to guide the puncture needle to remove the biopsy sample, or implant radioactive seeds through the needle. Besides, an electromagnetic position sensor attached to the US probe which will help to register the probe's working space to the MRI 3D reconstruction space that will be introduced in detail in the next section. The surgical robot will help surgeons to take the prostate brachytherapy surgery more stably.

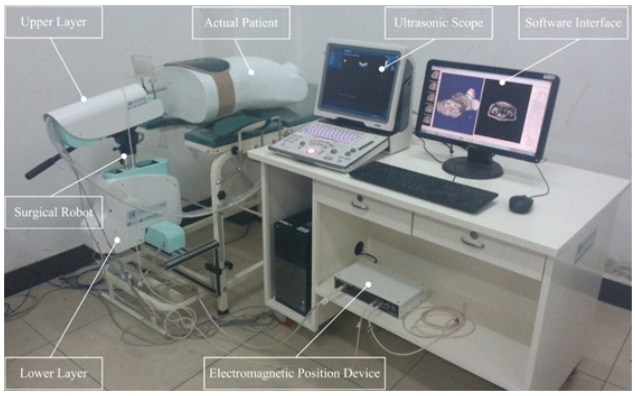

Figure 1. The general layout of the robotic prostate brachytherapy system.

The second part is the IGBS system that contains three main parts: 3D organs reconstruction, 3D conformal dose planning and US navigation. In order to make full use of open-source packages and build a surgical navigation system, the visualization toolkit (VTK) and the insight toolkit (ITK) are employed for image visualization and image registration respectively. The custom VTK classes are also used to acquire 3D position tracking information and 2D US images. In the navigation module, every component including image registration, US image acquisition and registered images visualization is integrated using multithreading techniques. After the US and MRI image registration, the quality of the US images will be improved by MRI images which can provide appropriate anatomical structure context. Then the surgeons can complete the prostate brachytherapy surgery more accurately.

Clinical workflow

The clinical workflow that we have designed for our system is illustrated in the block diagram in Figure 2. At the beginning of the procedure, an innovative registration method with frame is used to register the ultrasound probe to the MRI 3D reconstruction space that could capture the US pros-

tate image which is very close to the corresponding MRI at the same position of the prostate. At the same time, the 3D conformal dose planning is made according to the pre-operation MRI images that will instruct the operators to make needle trajectory planning.

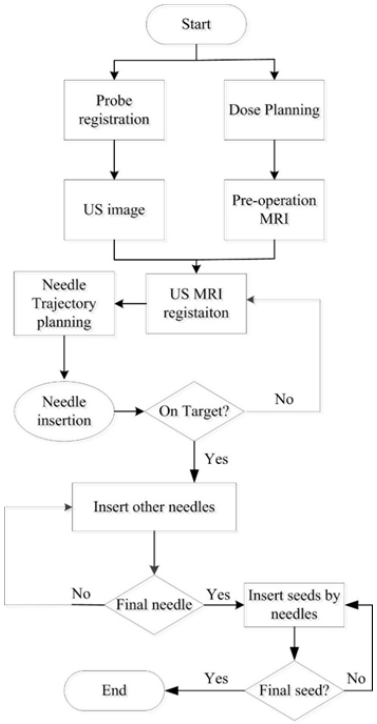

Figure 2. The clinical workflow.

After the probe registration, the US images captured in real-time are registered to pre-operation MRI images which together with the 3D conformal dose planning help the surgeons to make needle trajectory planning. In this process a deformable non-rigid image registration method was used to register the US images to MRI images which can reach a reasonable accuracy and speed. Then, with the help of the registered image, the locating needle according to the dose planning and trajectory planning was first inserted into the target and after the locating needle other needles were inserted.

Once the clinician is satisfied with the final needle position, the seeds are inserted, while progressively removing the needle. A 3D US volume may be acquired to check the position of each seed separately or globally for all seeds inserted by a needle. This procedure is repeated until all seeds have been distributed in the prostate

US probe registration

Registration of US images to MRI images is a complex process in medical image processing. Traditionally, in order to register US images to MRI images fast and accurately, an initial registration is usually made by the operators that puts the US images space position to the corresponding space position of the MRI images. This process usually costs a lot of time and is repeated many times by an experienced physician. We proposed an innovative registration method to improve this process by registering US probe to MRI 3D space in order to realize the automatic initial registration about US and MRI. This process describes a coordinates transformation, from a coordinate system defined in the pre-operatively acquired image data (image or virtual model space), into a coordinate system defined by the localizer which is located in the left of the surgical robot (actual or patient space) [34].

At present, popular registration can be described as following: both P and Q are referential Cartesian coordinates, which can be defined as either image space or physical space of instrument and navigation localizer. The goal of registration between both P and Q is to find out a transformation matrix ${}^{P}M_{Q}$, which enables the elements of both P and Q (p_P and p_Q) satisfy an expression:

$$\min \sum_{i=1}^{n} \left\| p_{P,i} - {}^{P}M_{\mathrm{Q}} \cdot p_{Q,i} \right\|^2 \qquad (1)$$

Currently, several methods of image-to-patient registration have been developed. Common methods include paired-point-based techniques with fiducial markers and surface-based registration using iterative closest point (ICP) [35].

In practical application, the number of the registration points is the main influence factor for the accuracy of ICP algorithm. If the number is large enough, the registration accuracy can satisfy the need of the clinical application. Too many points not only complicate the registration process but also expend the surgeons' more time and energy. To deal with these problems, an innovative concept called preoperative registration based on ICP is proposed, which makes use of a registration frame to obtain the positions of real and virtual registration points preoperatively. As a result of preoperative registration, a standard registration transformation matrix M_{inn} is obtained [36]. This transformation matrix M_{inn} can be used as the registration matrix in the progress of navigation, surgery and surgeons don't need to repeat the complicated registration process. They just need to get more than three additional paired-points, which can ensure that the relative position between the real and virtual patient are corresponding.

The calculations of the method are as follows: Firstly, pairs of corresponding points ${}^{inn}p_{act}$ and ${}^{inn}p_{mod}$ which act as registration points in the innovative registration method are obtained with the indentations of registration frame in actual and model space. Then as a result of innovative registration, a transformation matrix M_{inn} is obtained [see calculation (2)]. During the surgery (as mentioned above), surgeons just need to get more than three additional paired-points, which can ensure that the relative position in image between patient and frame are corresponding. Then a series of corresponding points ${}^{add}p_{act}$ and ${}^{add}p_{mod}$, which attached to the phantom's skin, are selected as additional registration points. The other points ${}^{add}p'_{mod}$ were gotten using ${}^{add}p_{act}$ multiplied by M_{inn} [see calculation (3)]. Points ${}^{add}p'_{mod}$ and ${}^{add}p_{mod}$ were used as correction points in the innovative registration, then an additional transformation matrix M_{add} between them was obtained

using the leastsquare method[see calculation (4)]. The rotation and translation parameters (α,β,γ) and (x,y,z) of M_{add} were solved through homogeneous equations. The position of virtual patient model will be adjusted automatically according to (α,β,γ) and (x,y,z) respectively when the calculations were performed. After that, the standard matrix can be used directly as registration result directly and the registration process was immensely simplified.

$$\min \sum_{i=1}^{n} \left\| {}^{\text{inn}}p'_{\text{mod}i} - M_{\text{inn}} \cdot {}^{\text{inn}}p_{\text{mod}i} \right\|^2 \quad (2)$$

$${}^{\text{add}}p'_{\text{mod}} = M_{\text{inn}} \cdot {}^{\text{add}}p_{\text{act}} \quad (3)$$

$$\min \sum_{i=0}^{n} \left\| {}^{\text{add}}p'_{\text{mod}i} - M_{\text{add}} \cdot {}^{\text{add}}p_{\text{mod}i} \right\|^2 \quad (4)$$

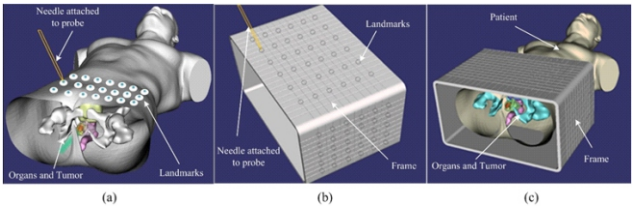

Figure 3. Experiments using registration frame, (a) The regular registration method experiment frame, (b) The innovative registration frame with a number of milled indentations at predefined locations is a polymethyl methacrylate (PMMA) cubic frame (c) The relative position of the frame and the patient.

In order to verify the effectiveness of innovative registration method, a registration frame is constructed, which serves as an artificial phantom for the experiments. The registration frame is a PMMA cubic frame, with a number of milled indentations at predefined locations across the frame's surface, which act as artificial landmarks points in the application [Figure 3(b)]. The diameter of the indentations matches exactly the diameter of the instrument's tip, allowing to precisely touch each of the points, which permitted us to perform an innovative preoperative registration combining with datum points on the abdominal cavity phantom's skin. The virtual model of the registration frame was used to get the virtual position of the registration points and was imported to our own navigation software through the STL format.

We also did experiments to compare our method comparing with the regular ICP method by using the frame shown in Figure 3. Results will be shown in the Results section.

Deformable registration method

After completing the probe registration, the initial registration of the US to MRI was performed at the same time. Then a deformable registration method is used to register US images to MRI in the intraprocedural registration process.

In this paper an alternative dependence measure proposed by Rényi(1959) [37] was used to replace MI as the measurement of the deformable registration method, which can deal with multi-modal image registration, but does not need the estimation of continuous joint probability density function. According to Rényi's theory, the maximum correlation coefficient MCC is chosen as the measurement which can satisfy the conditions proposed in the theory. Maximum correlation coefficient defined as follows.

$$\text{MCC}(X,Y) = \sup_{f,g \in V} \text{CC}(f(X), g(Y)) \quad (5)$$

Where f and g are Borel measurable functions and V is the space of the functions. MCC $(f(X), g(Y))$ is the correlation coefficient of $f(X)$ and $g(Y)$.

$$\text{CC}(f(X), g(Y)) = \frac{\text{Cov}(f(X), g(Y))}{\sqrt{\text{Var}(f(X))}\sqrt{\text{Var}(g(Y))}} \quad (6)$$

where Var and Cov are on behalf of variance and covariance, respectively.

Let $S(x)$ and $T(x)$ be the source image and target image on the image domain Ω, respectively, and $u(x)$ be the deformation field that deforms $S(x)$ to $T(x)$. So we used the theory of reproducing kernel Hilbert space (RKHS) to estimate the MCC between the deformed image $s_u(x) = s(x+u(x))$and target image $T(x)$. We choose to use the following Gaussian kernel:

$$K_\delta(x,y) = \frac{1}{\sqrt{2\pi}\delta} \exp\left\{ -\frac{(x-y)^2}{2\delta^2} \right\} \quad (7)$$

Let $S_u^f(x)$ and $T^g(x)$ be defined as:

$$S_u^f = \sum_{i=1}^{m} \alpha_i K_\delta(S_u(x), \xi_i), \; T^g(x) = \sum_{i=1}^{m} \beta_i K_\delta(T(x), \eta_i) \quad (8)$$

Then,

$$\text{MCC}(S_u, T) = \sup_{f,g} \text{CC}(S_u^f, T^g) \quad (9)$$

Now we can register the image $S(x)$ to $T(x)$ by solving the following minimization problem with respect to the deformation field $u(x)$:

$$\min_{u,\alpha,\beta} \lambda \int_\Omega |\nabla u(x)|^2 dx + |\Omega|(1 - \text{MCC}(S_u, T))^p \quad (10)$$

In this paper an iterative algorithm was used to find the minimizer $u(x)$, α, β to complete the registration between US and MRI images. The registered US and MRI images together with 3D reconstructed organs and the robotic system will help the surgeons to make the brachytherapy surgery more commodiously and accurately.

In order to assess the accuracy of the registration method,

five patients' MRI and US images were studied. All five patients had early prostate cancer and satisfied the condi-tions for prostate brachytherapy and surgery: PSA<10ng/ mL, T2 stage or Gleason grade ⩾8 points. Besides, multithre-ading and GPU techniques were also used in the IGBS sys-tem to increase the calculating speed. After the registration of MRI and US images of the prostate, the target registration error (TRE) (see calculation 11) was employed to verify the registration accuracy.

$$\mathrm{TRE} = \sqrt{\frac{1}{\mathrm{N}}\sum_{i=1}^{N}\left\|P_{MRi} - P_{USi}\right\|^2} \qquad (11)$$

P_{MRi} and P_{USi} are the points of landmarks on the MRI and US images respectively.

Results

In our navigation system, the position accuracy of the robot, errors between the rigidly connected robotic needle manipulator and electromagnetic tracker, the registration accuracy of the US probe registration and US-MRI registration are the main influence factors of the whole navigation system. Thus, experiments were performed to test and increase the accuracy of the navigation system.

Robotic accuracy

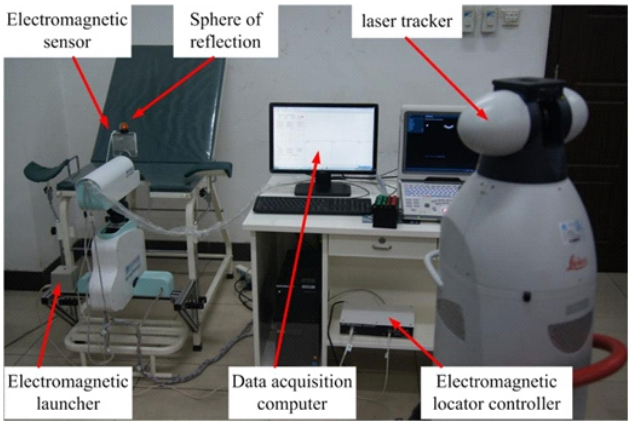

Figure 4. The instruments and equipment for repeatability test and electromagnetic tracer calibration.

The robot prototype has been built and is shown in Figure 1. The repeatability of positioning platform and the accuracy of the registration were tested and electromagnetic tracker calibration was carried out. A probabilistic experiment on repeatability was carried out to ensure the capacity of the robot in multiplying approaching different targets within the workspace and minimum range of error(less than 1mm). Here, we did a quantitative study on the accuracy of three leading screws. To this aim, a LASER tracker system (Leica-AT901-LR) was used to measure the positions of the end-effector of the robot. The reported accuracy of the measurement system is precision (was 0.016mm) enough to require for such a medical application.

As the end-effector of the robot system, the ultrasound probe and the needle guided module were positioned by electromagnetic tracker, and the precision of the electromagnetic tracker largely affected the system performance, so electromagnetic tracer calibration was carried out, as shown in Figure 4. The electromagnetic sensor was mounted on end-effector with sphere of reflection of the LASER tracker system. The positional information could be acquired from the electromagnetic tracer and the LASER tracker system when the end-effector was located in different positions. Comparing positional information between electromagnetic tracer and LASER tracker, the program of the electromagnetic tracer was modified to offset the error. Figure 5 shows the results (maximum error 0.4 mm) of the calibration.

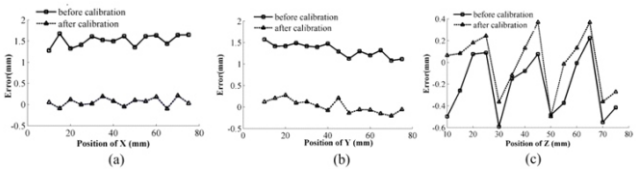

Figure 5. (a), (b) and (c) represent positional accuracy of X, Y and Z axes before and after calibration.

The errors shown in Figure 5 (a) and (b) obviously prove the validity of the calibration. The error in in Figure 5 (c) could be the cause of the deviation of the electromagnetic tracer itself. Thus, the accuracy of the robot system improved in an acceptable range.

Result of the US probe registration

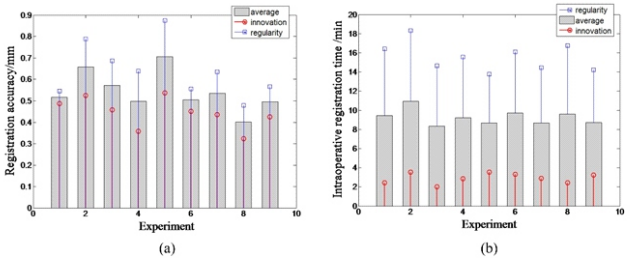

Figure 6. Experiment result of registration, (a) Accuracy of regular and innovative registration, (b) Time of regular and innovative registration.

In the experiments of the US probe registration, 90 landmark points, which should encircle the tumor of prostate, were collected on the abdominal surface to test the registration method. The accuracy of regular registration using phantom landmarks was 0.64±0.23mm. While the innovative registration with the points on frame surface, which also using 90 landmarks, reached an accuracy of 0.44±0.12 mm [see Figure 6(a)].

When the experiments of regular registration were conducted, the positions of landmarks on the phantom's sur-

face were obtained intraopetatively. However, during the experiments of innovative registration, the positions of landmarks on the frame's surface were obtained by developers of surgery navigation system preoperatively. So the surgeon just needed to collect a few of additional paired-points and click the button. A higher registration precision intraopetatively will be thus gained. The intraoperative times of regular registration and innovative registration were 16±2min and 3±1min [Figure 6 (b)].

Registration results

The MR and US images used in the experiments were from five patients. Note that all patients gave written informed consent for our research. The deformable registration process was executed offline after acquiring the US and MRI images. The satisfactory registration result was chosen to be shown in Figure 7.

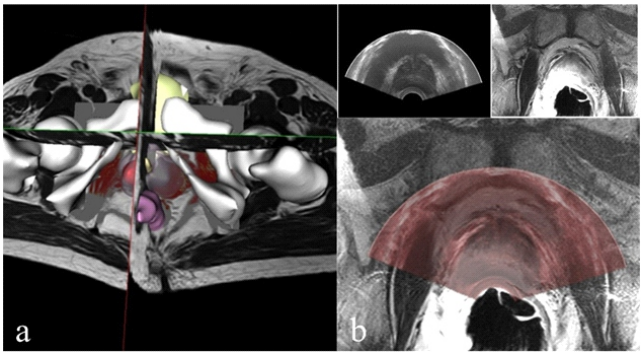

Figure 7. Registration result of 3D MR (gray) and 2D US (red) images of the prostate. (a) Registered 3D MR and 2D US images in 3D view. (b) The registration result of registering US and MR images in 2D view.

Evaluating the image registration accuracy of the prostate is incredibly difficult because prostate has few identifiable landmarks. Moreover, sometimes there are not enough landmarks to be selected to assess the registration accuracy needed for the characteristics of ultrasonic images (view limitation and low quality). In this paper, each captured US image was checked carefully by an experienced doctor of urology who chose the anatomical structures such as the urethra, lesions in the central gland or the center of tumors as landmarks (Figure.8).

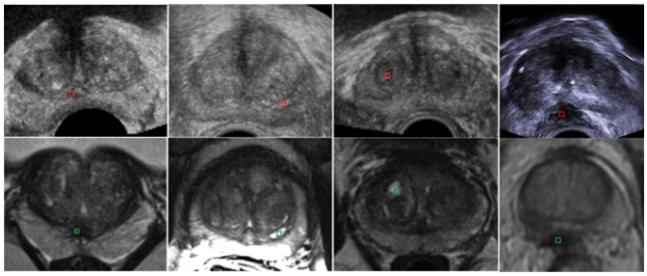

Figure 8. Landmarks in the images.

When the registration was completed, the TRE was calculated and the mean ± SD was 2.30±0.41mm. Compared with the MI based deformation registration method, the accuracy of the MCC-based registration method is better. The TRE is shown in Figure. 9.

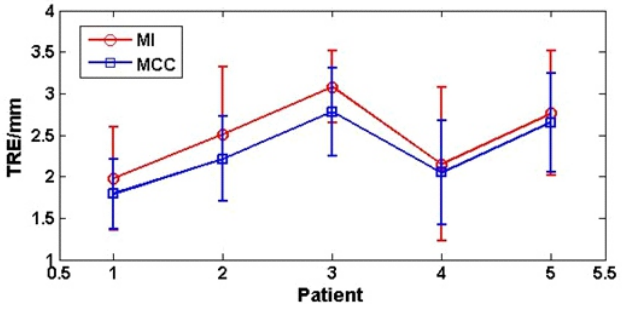

Figure 9. The TRE of the registration results.

Discussion

An ultrasound image navigation robotic prostate brachytherapy system based on US to MRI deformable image registration method is proposed in this paper. After the calibration of the robot system, the robot can provide stable and accurate US probe motion. With the help of the US probe registration, the initial registration of the US to MRI reached a high accuracy. Then an MCC-based multimodality image deformable registration method is proposed to register US to MR images which can make up for the lack on the vision during interventional procedures of prostate brachytherapy surgical. By using this robotic system, the quality of intraoperative US images was observably improved by the MR images which can provide high quality anatomical context. Even though the multiparametric (mpMRI) [38] and MRI [39] can supply excellent soft-tissue contrast which can guide the brachytherapy surgery accurately, it is very difficult to use them as a real-time navigation method for their complex circumstance and high cost. The intensive use of TRUS imaging plus MRI can improve the treatment planning for brachytherapy [40], but compared with the method described in this paper, without considering the deformation of the prostate made it less accurate than the deformation registration. In short, our system has potential to be widely applied. However, there are several aspects that still need to be optimized in this robotic system. In the US probe registration section, even though the accuracy and the cost of time were well improved, the registration process is still a little complex. Besides, the landmarks used to assess registration accuracy are sometimes difficult to find them out in the US/MR images. In the future, we will choose another method to simplify the process of the US registration and insert or attach some fiducial markers to the pros-tate to make them easier to be identified in US/MR images.

The final results of the US to MRI registration show that: compared with the MI-based deformable registration method (TRE is 2.50±0.45mm) the accuracy of the MCC-based deformable registration method (TRE is 2.30±0.41mm) was better in patients' studies. At the same time, the speed of convergence for the MCC-based method was faster than MI-

based method (shown in Figure 10). So if the MCC-based registration method is used in real-time US image registration, the duration of procedure may decrease a lot.

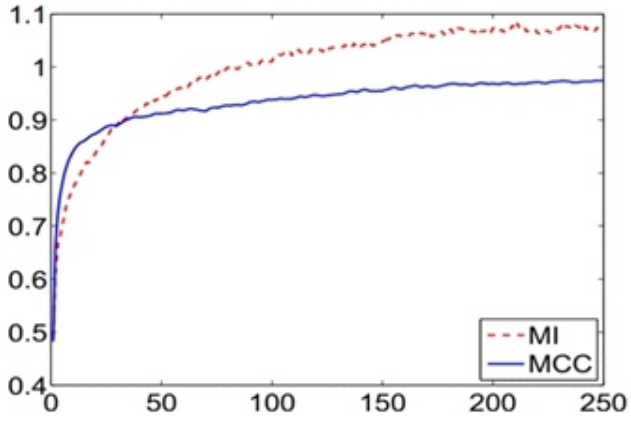

Figure 10. The results of iteration convergence for the MI and MCC

In conclusion, we have demonstrated an US image navigation robotic system which combined the US probe registration and MCC-based deformable registration method and proved its technical feasibility in prostate brachytherapy surgical. The technique proposed in this paper also has the latent energy to virtually improve the image guided navigation for other minimally invasive surgery just like radiofrequency ablation. The diagnostic capabilities for prostate cancer can also be improved through MR and US image registration and fusion. In the future, we will design another robotic system which will control needles directly replace the template to insert radioactive seeds and improve real-time registration.

Acknowledgment

We gratefully acknowledge our research team at the Center for Advanced Mechanisms and Robotics, Tianjin University and the help of the Tianjin Institute of Urology& Department of Urology, Second Hospital of Tianjin Medical University. This research was partly supported by the Education Program for New Century Excellent Talents (NCET-10-0625), Key Technology and Development Program of the Tianjin Municipal Science and Technology Commission (14ZCDZGX00490). No potential conflicts of interest were disclosed.

Bibliography

1. Siegel R, Ma JM, Zou ZH et al. Cancer Statistics, 2014. *Ca-a Cancer J. for Clinicians* 2014; 64: 9-29.
2. Buzurovic I, Podder TK, Yu Y. Prediction control for brachytherapy robotic system. *Journal of Robotics* 2010; 2010: ID 581840, 1-10
3. Buzurovic I, Podder T K, Yu Y. Robotic Systems for Radiation Therapy[M]. *INTECH Open Access Publisher*, 2012.
4. Yan KG, Podder T, Yu Y et al. Flexible needle–tissue interaction modeling with depth-varying mean parameter: preliminary study. *Biomedical Engineering, IEEE Transactions on* 2009; 56: 255-62.
5. Fu L, Liu H, Brasacchio R et al. Clinical Observation and Modeling of Postimplant Seed Displacement for Prostate Brachytherapy. *Int J Rad Onco* Biol* Phys* 2005; 63: S504-S5.
6. Ng W, Chung V, Vasan S et al., editors. Robotic radiation seed implantation for prostatic cancer. Engineering in Medicine and Biology Society, 1996 Bridging Disciplines for Biomedicine Proceedings of the 18th Annual International Conference of the IEEE; 1996: IEEE.
7. Meltsner M, Ferrier NJ, Thomadsen B. Observations on rotating needle insertions using a brachytherapy robot. *Phys Med Biol* 2007; 52: 6027-6037
8. Fichtinger G, Fiene J, Kennedy CW et al. Robotic assistance for ultrasound guided prostate brachytherapy. Medical Image Computing and Computer-Assisted Intervention–MICCAI 2007: Springer; 2007. p.119-27.
9. Fichtinger G, Fiene JP, Kennedy CW et al. Robotic assistance for ultrasound-guided prostate brachytherapy. *Med Image Analysis* 2008; 12: 535-45.
10. Krieger A, Iordachita II, Guion P et al. An MRI-compatible robotic system with hybrid tracking for MRI-guided prostate intervention. *Biomed Engineer, IEEE Transactions on* 2011; 58: 3049-60.
11. Hill DLG, Batchelor PG, Holden M et al. Medical image registration. *Phys Med Biol* 2001; 46: R1-R45.
12. Crum WR, Hartkens T, Hill DLG. Non-rigid image registration: theory and practice. *Brit J Radiol* 2004; 77: S140-S53.
13. Brock KK, Sharpe MB, Dawson LA et al. Accuracy of finite element model-based multi-organ deformable image registration. *Med Phys* 2005; 32: 1647-59.
14. Lu WG, Olivera GH, Chen Q et al. Automatic re-contouring in 4D radiotherapy. *Phys Med Biol* 2006; 51: 1077-99.
15. Rietzel E, Chen GTY. Deformable registration of 4D computed tomography data. *Med Phys* 2006; 33: 4423-30.
16. Chao M, Xie YQ, Xing L. Auto-propagation of contours for adaptive prostate radiation therapy. *Phys Med Biol* 2008; 53: 4533-42.
17. Wang H, Adam SG, Zhang LF et al. Performance evaluation of automatic anatomy segmentation algorithm on repeat or four-dimensional computed tomography images using deformable image registration method. *Int J Radiat Oncol* 2008; 72: 210-9.
18. Xie YQ, Chao M, Lee P et al. Feature-based rectal contour propagation from planning CT to cone beam CT. *Med Phys* 2008; 35: 4450-9.
19. Wu GR, Wang Q, Lian J et al. Reconstruction of 4D-CT from a Single Free-Breathing 3D-CT by Spatial-Temporal Image Registration. *Lect Notes Comput Sc* 2011; 6801: 686-98.
20. Ren L, Chetty IJ, Zhang J et al. Development and clinical evaluation of a three-dimensional cone-beam computed tomography estimation method using a deformation field map. *Int J Radiat Oncol* Biol* Phys* 2012; 82: 1584-93.
21. Yan D, Jaffray DA, Wong JW. A model to accumulate fractionated dose in a deforming organ. *Int J Radiat Oncol* 1999; 44: 665-75.
22. Rietzel E, Chen GT, Choi NC et al. Four-dimensional image-based treatment planning: Target volume segmentation and dose calculation in the presence of respiratory motion. *Int J Radiat Oncol* Biol* Phys* 2005; 61: 1535-50.
23. Keall PJ, Joshi S, Vedam SS et al. Four-dimensional radiotherapy planning for DMLC-based respiratory motion tracking. *Med Phys 2005; 32: 942-51.*
24. Boldea V, Sharp GC, Jiang SB et al. 4D-CT lung motion estimation with deformable registration: Quantification of motion nonlinearity and hysteresis. *Med Phys* 2008; 35: 1008-18.
25. Ehrhardt J, Werner R, Saring D et al. An optical flow based method for improved reconstruction of 4D CT data sets acquired during free breathing. *Med Phys* 2007; 34: 711-21.
26. Yang DS, Lu W, Low DA et al. 4D-CT motion estimation using deformable image registration and 5D respiratory motion modeling. *Med Phys* 2008; 35: 4577-90.
27. Zeng RP, Fessler JA, Balter JM. Estimating 3-D respiratory motion from orbiting views by tomographic image registration. *IEEE T Med Imaging* 2007; 26: 153-63.

28. Kim J, Hammoud R, Pradhan D et al. Prostate Localization on Daily Cone-Beam Computed Tomography Images: Accuracy Assessment of Similarity Metrics. *Int J Radiat Oncol* 2010; 77: 1257-65.
29. Kim J, Kumar S, Liu C et al. A novel approach for establishing benchmark CBCT/CT deformable image registrations in prostate cancer radiotherapy. *Phys Med Biol* 2013; 8: 8077-97.
30. Gu XJ, Dong B, Wang J et al. A contour-guided deformable image registration algorithm for adaptive radiotherapy. *Phys Med Biol* 2013; 58: 1889-901.
31. Schreibmann E, Xing L. Image registration with auto-mapped control volumes. *Med Phys* 2006; 33: 1165-79.
32. Xu S, Kruecker J, Turkbey B et al. Real-time MRI-TRUS fusion for guidance of targeted prostate biopsies. *Comput Aided Surg* 2008; 13: 255-64.
33. Zhang SH, Jiang S, Yang ZY et al. 2D Ultrasound and 3D MR Image Registration of the Prostate for Brachytherapy Surgical Navigation. *Medicine* 2015; 94: e1643(1-10).
34. Schmitz AC, Gianfelice D, Daniel BL et al. Image-guided focused ultrasound ablation of breast cancer: current status, challenges, and future directions. *Eur Radiol* 2008; 18: 1431-41.
35. Wiles AD, Peters TM. Real-Time Estimation of FLE Statistics for 3-D Tracking With Point-Based Registration. *IEEE T Med Imaging* 2009; 28: 1384-98.
36. Spinczyk D, Karwan A, Copik M. Methods for abdominal respiratory motion tracking. *Comput Aided Surg* 2014; 19: 34-47.
37. Rényi A. On measures of dependence. *Acta Mathematica Academiae Scientiarum Hungaricae* 1959; 10: 441-51.
38. Nicolae A M, Venugopal N, Ravi A. Trends in targeted prostate brachytherapy: from multiparametric MRI to nanomolecular radiosensitizers. *Cancer Nanotechnology* 2016; 7: 1-17.
39. Kuo N, Lee J, Tempany C, et al. Mri-based prostate brachytherapy seed localizati. *2010 IEEE International Symposium on Biomedical Imaging: From Nano to Macro. IEEE* 2010: 1397-400.
40. Reynier C, Troccaz J, Fourneret P, et al. MRI/TRUS data fusion for prostate brachytherapy. Preliminary results. *Medical Physics* 2004, 31: 1568-75.

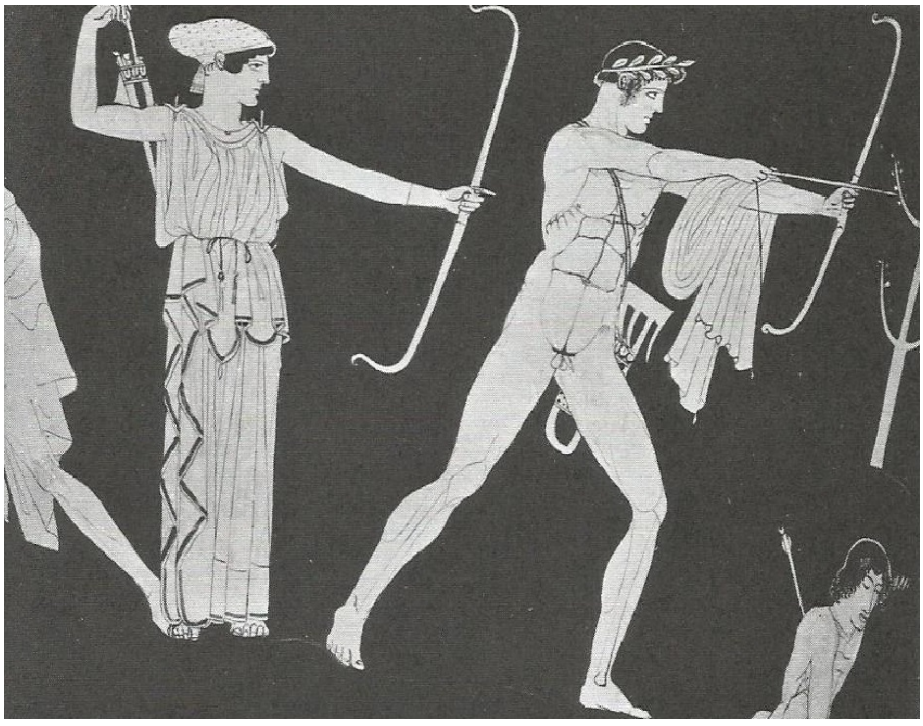

Apollo and Artemis are killing the children of Niovi. Niovi mocked Lito, the mother of Artemis and Apollo, publicly and her children decided to take revenge for this assault.